A discontinuity in mantle composition beneath the southwest Indian ridge

Christine M. Meyzen*†, Michael J. Toplis*, Eric Humler‡, John N. Ludden* & Catherine Mével‡

** Centre de Recherches Pétrographiques et Géochimiques (CRPG), UPR 2300, 15 rue Notre-Dame-des-Pauvres, BP 20, 54501 Vandoeuvre-Les-Nancy, France*
‡ Laboratoire de Geosciences Marines, Institut de Physique du Globe (IPG), 4 place Jussieu, 75251 Paris cedex 05, France
† Present address: Danish Lithosphere Centre, Øster Voldgade 10, 1350 Copenhagen, Denmark

The composition of mid-ocean-ridge basalt is known to correlate with attributes such as ridge topography[1,2] and seismic velocity in the underlying mantle[3], and these correlations have been interpreted to reflect variations in the average extent and mean pressures of melting during mantle upwelling. In this respect, the eastern extremity of the southwest Indian ridge is of special interest, as its mean depth of 4.7 km (ref. 4), high upper-mantle seismic wave velocities[5] and thin oceanic crust of 4–5 km (ref. 6) suggest the presence of unusually cold mantle beneath the region. Here we show that basaltic glasses dredged in this zone, when compared to other sections of the global mid-ocean-ridge system, have higher $Na_{8.0}$, Sr and Al_2O_3 compositions, very low CaO/Al_2O_3 ratios relative to TiO_2 and depleted heavy rare-earth element distributions. This signature cannot simply be ascribed to low-degree melting of a typical mid-ocean-ridge source mantle, as different geochemical indicators of the extent of melting[1] are mutually inconsistent. Instead, we propose that the mantle beneath ~1,000 km of the southwest Indian ridge axis has a complex history involving extensive earlier melting events and interaction with partial melts of a more fertile source.

This study reports the major- and trace-element compositions of basaltic glasses dredged along the southwest Indian ridge (SWIR) between 49° and 69° E during the EDUL cruise (Fig. 1, Supplementary Table 1). Although this entire section of ridge axis is characterized by extremely low spreading rate (full spreading rate, 11–15 mm yr^{-1})[7], it may be divided (on the basis of geophysical characteristics) into two zones separated by the Melville fracture zone (MFZ) at 60° 45′ E. To the east of the MFZ (zone A, Fig. 1) the ridge displays the extreme geophysical characteristics described above, while to the west of the MFZ (zone B, Fig. 1), the axial segmentation pattern is smoother and mean axial depth ranges from 4,330 to 3,090 m going from east to west.

Sample compositions have Mg number (Mg# = 100Mg/(Mg + Fe)) in the range 0.49–0.66, although most of the compositions located to the east of the MFZ are relatively undifferentiated (Mg# > 0.58). When compared at similar MgO contents, the major-element chemistry of basaltic glasses from zone A is systematically distinct from all previously described mid-ocean-ridge basalt (MORB; Supplementary Table 1). For example, these lavas

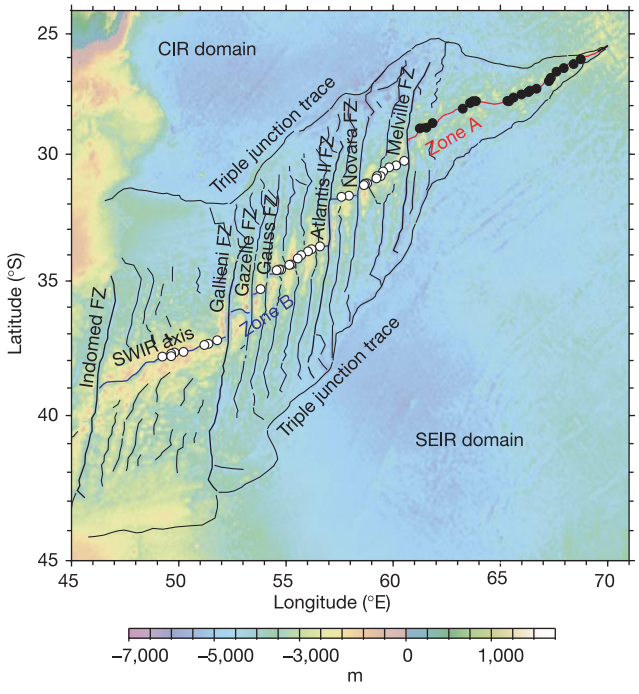

Figure 1 Topographic map of the southwest Indian ridge (SWIR), showing sample locations used in this study (circles). (Map is from ref. 21.) The SWIR is propagating at about twice its spreading rate[22] at the Rodriguez triple junction, where the central Indian ridge (CIR) joins also the southeast Indian ridge (SEIR). FZ, fracture zone.

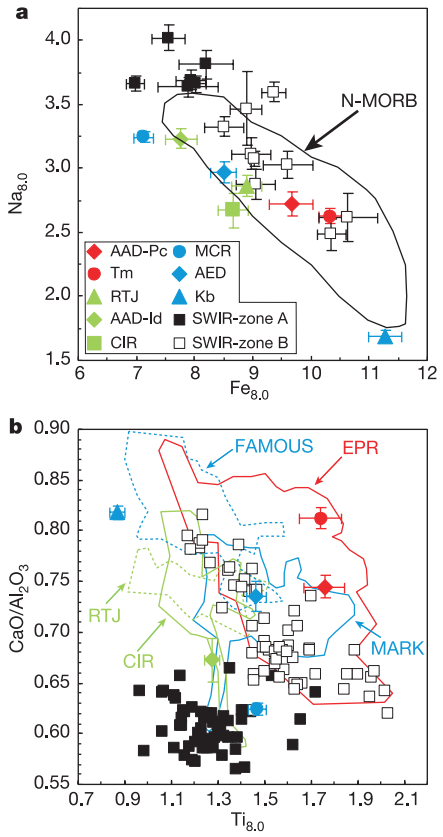

Figure 2 Characteristics of the major-element chemistry of SWIR lavas compared to those from other mid-ocean ridges. **a**, $Na_{8.0}$ versus $Fe_{8.0}$, and **b**, CaO/Al_2O_3 versus $Ti_{8.0}$. The subscript 8.0 indicates that oxides have been corrected to MgO = 8% (refs 1, 2). $Na_{8.0}$ and $Fe_{8.0}$ have been averaged over mean ridge length of 60 ± 30 km. Outlined fields are for normal MORB (N-MORB)[2], East Pacific Rise (EPR), MARK, FAMOUS areas, central Indian ridge (CIR) and Rodriguez triple junction (RTJ). Also shown are averages from the Mid-Cayman rise (MCR), Indian and Pacific sides of the Australian–Antarctic discordance (AAD-Id and AAD-Pc respectively), Atlantic equatorial discordance (AED), Tamayo (Tm) region of the EPR, RTJ, CIR and Kolbeinsey ridge (Kb). Only data from the two deepest ridge segments of the AED are used. Error bars are 2σ. See Supplementary Information for references used.

define the highest reported values of $Na_{8.0}$ at low values of $Fe_{8.0}$ in the global array[1] (Fig. 2a). In contrast, basalts from zone B fall in the global array of $Na_{8.0}$ versus $Fe_{8.0}$. Here and elsewhere the subscript 8.0 refers to values corrected for low-pressure fractionation to a common MgO content of 8wt%, as described by ref. 1.

Basalts from zone A are also distinguished by their consistently high Al_2O_3 (16.1–18.3 wt%) and low $Ti_{8.0}$, as illustrated by the co-variation of CaO/Al_2O_3 and $Ti_{8.0}$ (Fig. 2b). Even if rare lavas with low CaO/Al_2O_3 and low $Ti_{8.0}$ have been previously identified in the Atlantic equatorial discordance[8], the MARK region[9] and the central Indian ridge[10], it is clear that zone A lavas systematically define a unique compositional field for MORB glasses. The mid-Cayman rise[11,12] and, to a lesser extent, the Indian side of the Australian–Antarctic discordance[13–15], two 'cold sections' of the global mid-ocean ridge system, also display mild offsets to low CaO/Al_2O_3 relative to $Ti_{8.0}$, as do the fields defined by the Rodriguez triple junction and the central Indian ridge. In contrast, MORB from zone B falls within the compositional array defined by North Atlantic lavas.

In terms of trace-element geochemistry, zone B glasses overlap trends defined by basalts from other mid-ocean spreading centres (see, for example, Fig. 3a). This is also true for highly incompatible elements such as $Ce_{8.0}$ in basalts of zone A. However, when compared as a function of $(Sm/Yb)_n$ (where the subscript n means chondrite normalized values), these lavas are found to be progressively depleted in trace elements of increasing compatibility, such that they have uniformly lower heavy rare-earth element (HREE) concentrations relative to basalts from zone B and to the global array (Fig. 3a). This offset is also a feature of the Indian side of the Australian–Antarctic discordance. Furthermore, consideration of $Na_{8.0}$ as a function of $(Sm/Yb)_n$ demonstrates that zone A lavas are highly enriched in sodium compared to all other ridges at a given value of $(Sm/Yb)_n$ (Fig. 3b). The same is true of Sr and Al_2O_3.

Although the co-variation of $Na_{8.0}$ and $Fe_{8.0}$ (Fig. 2a) could justifiably lead to the inference that zone A basalts may be explained by extremely low extents of mantle melting at low mean pressure, consideration of all major and trace elements shows that this simple scheme is untenable. For example, during partial melting of a clinopyroxene-bearing source the $(Sm/Yb)_n$ of liquids should also be an indicator of the extent of partial melting[1]. However, although basalts from zone B show the same correlation between $Na_{8.0}$ and $(Sm/Yb)_n$ as that defined by other spreading centres, this is clearly not the case for zone A lavas (Fig. 3b). Furthermore, as partial melting of a clinopyroxene-bearing source proceeds, the CaO/Al_2O_3 of liquids increases while TiO_2 decreases, leading to the co-variation observed for zone B lavas and the vast majority of lavas from the global array (Fig. 2b). Lavas from zone A are obviously inconsistent with this general trend, suggesting that a lower-than-normal degree of partial melting of a typical mantle source is not responsible for their unique geochemistry.

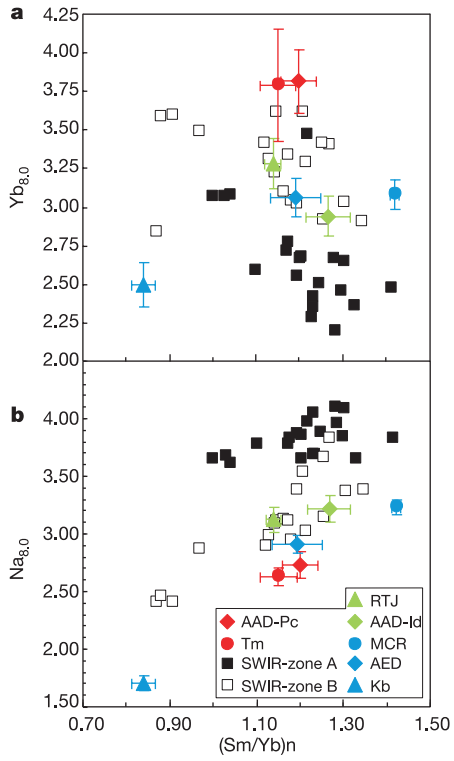

Figure 3 Variations of major- and trace-element chemistry of SWIR lavas compared to those from other mid-ocean ridges. $Yb_{8.0}$ (**a**) and $Na_{8.0}$ (**b**) versus $(Sm/Yb)_n$. Symbols as in Fig. 2. To avoid effects of low-pressure fractional crystallization, REE contents have been corrected to 8 wt% MgO. This correction is based on the calculation of $Ce_{8.0}$ from ref. 23, and assuming that all REE have a partition coefficient of zero during low-pressure fractionation.

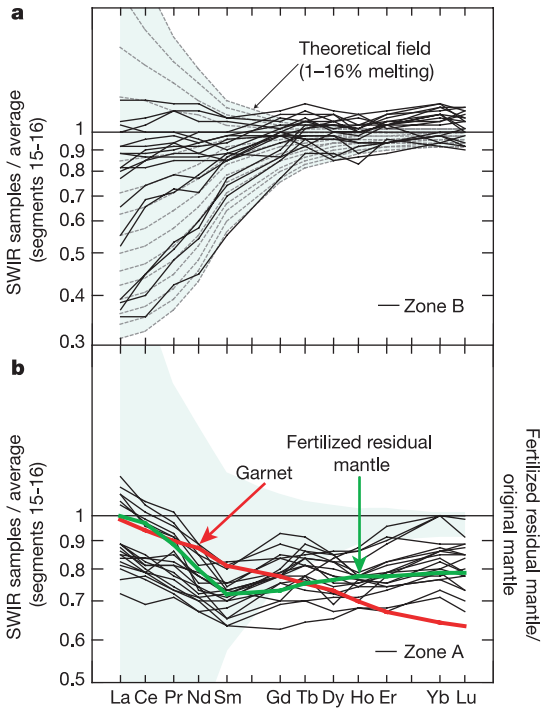

Figure 4 Rare-earth element systematics of glasses from zones B and A. **a**, Zone B; **b**, zone A. REE corrected to 8 wt% MgO, and normalized to the average glass composition from the two ridge segments immediately west of the MFZ. Grey dotted lines in **a** represent theoretical curves for non-modal near fractional melting at 1.2% melting per kbar (ref. 2) normalized to the theoretical liquid produced at ~5% melting. The red line in **b** represents 5% melting with half the melting in the garnet stability field normalized to a liquid produced by 5% melting in the spinel stability field only. The green line ('fertilized residual mantle') corresponds to the relative composition (compared to the original source) of a mantle having undergone 10% melting, then fertilized by 5 relative per cent of a liquid produced by ~5% melting. This curve is only directly comparable to that of the normalized glass data if it is assumed that the degree of melting of the refertilized source is the same as that of the composition used to normalize the glass data. Even so, other degrees of melting of the refertilized source produce qualitatively similar profiles. Any secondary clinopyroxene crystallized during fertilization will be low enough in abundance to be completely eliminated during remelting. Further details are given in Supplementary Information.

In order to constrain the origin of zone A basalts, we will concentrate on the rare-earth elements (REE), as relative fractionations between these elements are known to provide a sensitive probe of the partial melting process. For example, the different compatibility of different REE in clinopyroxene leads to a pronounced relative depletion in the light REE (LREE) in the liquids as melting proceeds, as illustrated in Fig. 4a for basalts from zone B. In this representation all liquid compositions have been corrected to 8 wt% MgO, then normalized to the average composition of glasses from the two ridge segments in zone B immediately to the west of the MFZ (Supplementary Table 4). First, this normalization eliminates the need to know the source composition as long as a single source is assumed. Second, this average was chosen because these segments reflect the lowest degree of partial melting from zone B (estimated to be ~6.7% of a typical normal-MORB source based on its $Na_{8.0}$ contents[2]), thus all other glasses from this zone should represent higher degrees of melting. As expected, normalized REE patterns are fan-shaped (Fig. 4a), with the most depleted compositions occurring at the western extremity of the zone, at the shallowest depths and having the lowest $Na_{8.0}$, $Ti_{8.0}$ and $(Sm/Yb)_n$, and highest $Fe_{8.0}$ and CaO/Al_2O_3; all of these melt proxies are consistent with a progressive increase in degree of partial melting of a fertile lherzolite from east to west in zone B.

In marked contrast, when zone A basalts are corrected to 8 wt% MgO and normalized to the same average composition, a completely different REE pattern is apparent (Fig. 4b). The normalized spectra are U-shaped, with a steep decrease in relative concentration from La to Sm then a slight positive slope from Sm to Yb. Another significant feature is that the spectra are all more or less parallel with little relative fractionation between REE as a function of absolute concentration, contrasting with zone B basalts (Fig. 4b). We note that the concentrations of the HREE are systematically depleted relative to the reference composition. From this representation, it is clear that basalts from zones A and B have not been produced by different degrees of partial melting of the same source. Melting in the garnet stability field, as has been previously suggested for this region[16,17], can also be excluded, as significant involvement of garnet would fractionate the HREE from the LREE, in contrast to our observations (Fig. 4b).

The parallel nature of the REE patterns in zone A (Fig. 4b) is inconsistent with the presence of clinopyroxene in the residue over the sampled melting interval. We note that this does not exclude the possibility that a small proportion of clinopyroxene was present at melt fractions lower than those sampled by the basalts. The inference that clinopyroxene was absent from the residue also provides an explanation for the observed correlation between CaO/Al_2O_3 and $Ti_{8.0}$ (Fig. 2b), because once clinopyroxene is exhausted during melting, experimental studies[18,19] have shown that CaO/Al_2O_3 of the liquid changes from increasing to decreasing values. Independent support for this idea is provided by peridotites dredged from zone A, which are notably poor in clinopyroxene[20]. The simplest way to produce a mantle depleted in clinopyroxene is for it to have undergone a prior partial melting event, a hypothesis consistent with the strong depletion in HREE (Fig. 4b). However, this simple model cannot explain the high concentrations of the more incompatible elements such as the LREE or Na, which should have been almost entirely removed from the source during the first melting event, and some re-fertilization of this depleted source is required. Although the exact nature of this contaminating liquid and its origin cannot be determined with certainty, the REE pattern of zone A liquids can be satisfactorily accounted for by mixture of a harzburgite and a partial melt of a fertile peridotite (Fig. 4b).

This interpretation begs the question of whether the SWIR has the attributes of a 'cold section' because mantle potential temperature is low, or because the mantle source is less fertile and thus less able to produce melt. Furthermore, it raises questions concerning the geodynamic origins of zone A basalts. Previous melting of the asthenosphere beneath the central Indian ridge may play a part (Fig. 1), but this cannot explain the fact that the mantle has been affected over distances of ~1,000 km. Alternatively these basalts may reflect melting of ultra-depleted asthenosphere that has been entrained into the ridge system and is floating above 'normal' asthenosphere. Such depleted sources may be a general feature of the Indian Ocean mantle, resulting in a different spectrum of source composition than present beneath the Atlantic and Pacific oceans. □

Received 9 September 2002; accepted 9 January 2003; doi:10.1038/nature01424.

1. Klein, E. M. & Langmuir, C. H. Global correlations of ocean ridge basalt chemistry with axial depth and crustal thickness. *J. Geophys. Res.* **92,** 8089–8115 (1987).
2. Langmuir, C. H., Klein, E. M. & Plank, T. in *Mantle Flow and Melt Generation at Mid-Ocean Ridges* (eds Phipps-Morgan, J., Blackmann, D. K. & Sinton, J. M.) 183–280 Geophysical Monograph series, Vol. 71 (American Geophysical Union, Washington DC, 1992).
3. Humler, E., Thirot, J. L. & Montagner, J. P. Global correlations of mid-ocean-ridge basalt chemistry with seismic tomographic images. *Nature* **364,** 225–228 (1993).
4. Cannat, M., Rommevaux-Jestin, C., Sauter, D., Deplus, C. & Mendel, V. Formation of the axial relief at the very slow spreading Southwest Indian Ridge (49°-69°E). *J. Geophys. Res.* **104,** 22825–22843 (1999).
5. Debayle, E. & Levêque, J. J. Upper mantle heterogeneities in the Indian Ocean from waveform inversion. *Geophys. Res. Lett.* **24,** 245–248 (1997).
6. Muller, M. R., Minshull, T. A. & White, R. S. Segmentation and melt supply at the Southwest Indian Ridge. *Geology* **27,** 867–870 (1999).
7. Shu, D. & Gordon, R. G. Evidence for motion between Nubia and Somalia along the Southwest Indian Ridge. *Nature* **398,** 64–66 (1999).
8. Schilling, J. G. *et al.* Thermal structure of the mantle beneath the Equatorial Mid-Atlantic Ridge: Inferences from the spatial variation of dredged basalt glass compositions. *J. Geophys. Res.* **100,** 10057–10076 (1995).
9. Bryan, W. B., Humphris, S. E., Thompson, G. & Casey, J. F. Comparative volcanology of small axial eruptive centers in the MARK area. *J. Geophys. Res.* **99,** 2973–2984 (1994).
10. Natland, J. H. in *Oceanic Basalts* (ed. Floyd, P. A.) 288–310 (Blackie and Son, Glasgow, 1991).
11. Elthon, D., Ross, D. K. & Meen, J. K. Compositional variations of basaltic glasses from the Mid-Cayman Rise spreading center. *J. Geophys. Res.* **100,** 12497–12512 (1995).
12. Elthon, D., Ross, D. K. & Meen, J. K. Correction to "Compositional variations of basaltic glasses from the Mid-Cayman Rise spreading center". *J. Geophys. Res.* **101,** 17577–17579 (1996).
13. Klein, E. M., Langmuir, C. H. & Staudigel, H. Geochemistry of basalts from the Southeast Indian Ridge 115°-138°E. *J. Geophys. Res.* **96,** 2089–2107 (1991).
14. Pyle, D. G., Christie, D. M., Mahoney, J. J. & Duncan, R. A. Geochemistry and geochronology of ancient southeast Indian and southwest Pacific seafloor. *J. Geophys. Res.* **100,** 22261–22282 (1995).
15. Pyle, D. G. *Geochemistry of Mid-ocean Ridge Basalt Within and Surrounding the Australian-Antarctic Discordance*. Thesis, Oregon State Univ. (1994).
16. White, R. S., Minshull, T. A., Bickle, M. J. & Robinson, C. J. Melt generation at very slow-spreading oceanic ridges: Constraints from geochemical and geophysical data. *J. Petrol.* **42,** 1171–1196 (2001).
17. Robinson, C. J., Bickle, M. J., Minshull, T. A., White, R. S. & Nichols, A. R. L. Low degree melting under the Southwest Indian Ridge: the roles of mantle temperature, conductive cooling and wet melting. *Earth Planet. Sci. Lett.* **188,** 383–398 (2001).
18. Pickering-Witter, J. & Johnston, A. D. The effects of variable bulk composition on the melting systematics of fertile peridotitic assemblages. *Contrib. Mineral. Petrol.* **140,** 190–211 (2000).
19. Falloon, T. J. & Danyushevsky, L. V. Melting of refractory mantle at 1.5, 2 and 2.5 GPa under anhydrous and H_2O-undersaturated conditions: Implications for the petrogenesis of high-Ca boninites and influence of subduction components on mantle melting. *J. Petrol.* **41,** 257–283 (2000).
20. Seyler, M., Cannat, M. & Mével, C. Evidence for major-element heterogeneity in the mantle source of abyssal peridotites from the Southwest Indian Ridge (52° to 68°E). *Geochem. Geophys. Geosyst.* (in the press).
21. Smith, W. H. F. & Sandwell, D. T. Global seafloor topography from satellite altimetry and ship depth soundings. *Science* **277,** 1957–1962 (1997).
22. Patriat, P., Sauter, D., Munschy, M. & Parson, L. A survey of the Southwest Indian Ridge axis between Atlantis P fracture zone and the Indian Ocean triple junction: regional setting and large-scale segmentation. *Mar. Geophys. Res.* **19,** 457–480 (1997).
23. Plank, T. & Langmuir, C. H. Effects of the melting regime on the composition of the oceanic crust. *J. Geophys. Res.* **97,** 19749–19770 (1992).

Supplementary Information accompanies the paper on *Nature*'s website (**http://www.nature.com/nature**).

Acknowledgements We thank the Service d'Analyse des Roches et des Minéraux (SARM) and J. Carignan for their help in the laboratory. We also thank D. Sauter for helpful discussions. Funding was provided by CNRS-INSU, and the IFRTP provided access to the Marion Dufresne II for sampling.

Competing interests statement The authors declare that they have no competing financial interests.

Correspondence and requests for materials should be addressed to C.M. (e-mail: cm@dlc.ku.dk).